

# Direct Interaction between Anthrax Toxin Receptor 1 and the Actin Cytoskeleton<sup>†</sup>

Kristopher M. Garlick and Jeremy Mogridge\*

*Department of Laboratory Medicine and Pathobiology, University of Toronto, Toronto, Ontario M5S 1A8, Canada*

*Received September 1, 2009; Revised Manuscript Received October 5, 2009*

**ABSTRACT:** The protective antigen component of anthrax toxin binds the I domain of the anthrax toxin receptors, ANT XR1 and ANT XR2, in a manner akin to how integrins bind their ligands. The I domains of integrins and ANT XR1 both have high- and low-affinity conformations, and the cytosolic tails of these receptors associate with the actin cytoskeleton. The association of ANT XR1 with the cytoskeleton correlates with weakened binding to PA, although a mechanistic explanation for this observation is lacking. Here, we identified a segment in the cytoplasmic tail of ANT XR1 required for its association with the cytoskeleton. We synthesized a 60-mer peptide based on this segment and demonstrated a direct interaction between the peptide and  $\beta$ -actin, indicating that in contrast to integrins, ANT XR1 does not use an adaptor to bind the cytoskeleton. This peptide orders actin filaments into arrays, demonstrating an actin bundling activity that is novel for a membrane protein.

Anthrax toxin consists of protective antigen (PA),<sup>1</sup> edema factor (EF), and lethal factor (LF). PA binds the anthrax toxin receptors, ANT XR1 and ANT XR2, and delivers the enzymatic components of the toxin, EF and LF, into the cell where they exert their toxic activities (1). EF is an adenylate cyclase, and LF is a zinc metalloprotease that cleaves most mitogen-activated protein kinase kinases (MAPKKs) (2, 3).

ANT XR1 and ANT XR2 are type I membrane proteins that exhibit a high degree of similarity (1). PA binds the extracellular von Willebrand Factor type A or integrin-inserted (VWA/I) domain of each receptor. The I domains also bind the natural ligands of the receptors: collagen type I and VI for ANT XR1 and laminin and collagen IV for ANT XR2 (4–6). The receptors are expressed widely, although their physiological functions have not been fully elucidated. Recently, however, it has been shown that ANT XR1 and ANT XR2 knockout female mice are unable to reproduce (7). Another study showed that ANT XR1 knockout mice accumulate excessive extracellular matrix in several tissues, including the ovaries and uterus (8). Mutations in ANT XR2 are associated with the human diseases juvenile hyaline fibromatosis and infantile systemic hyalinosis, which are characterized by the accumulation of extracellular matrix and contractures of the joints (9). Cumulatively, these results suggest that the receptors are cell adhesion molecules involved in extracellular matrix homeostasis.

ANT XR1 has been shown to mediate cell spreading on collagen I by a process that is dependent on an interaction between its cytoplasmic tail and the actin cytoskeleton (10). We previously demonstrated that the linkage between the cytoplasmic

domain of ANT XR1 and the actin cytoskeleton affected the binding of PA (11). Cells that expressed a splice variant of ANT XR1 that associated with actin [splice variant 1 (sv1)] bound markedly less PA than cells that expressed a shorter variant that did not associate with actin (sv2) (11). In addition, introduction of the Y383C point mutation into the cytoplasmic tail of ANT XR1-sv1, which is synonymous with a disease-causing mutation in ANT XR2, disrupted receptor–cytoskeleton association and strengthened the binding of PA (11). These results suggest that ANT XR1 possesses different affinity states that may be modulated by cytoplasmic interactions. This notion is reminiscent of what has been observed for integrins, which can shift from low- to high-affinity conformations as a result of how adaptor proteins interact with their cytoplasmic tails (12).

Here we have delimited a short region within the ANT XR1 cytoplasmic domain required for its association with the cytoskeleton. We synthesized a peptide based on this region and found that it interacted with  $\beta$ -actin in HeLa cells. Furthermore, this peptide bound to purified monomeric  $\beta$ -actin *in vitro*, indicating that the interaction between ANT XR1 and the actin cytoskeleton is direct. In addition, we show that ANT XR1 is capable of organizing actin filaments into bundles.

## EXPERIMENTAL PROCEDURES

**Cell Culture.** HeLa cells were maintained in HG-DME medium supplemented with 10% fetal bovine serum (Invitrogen) and 1  $\times$  penicillin-streptomycin. HeLa cells were transfected with polyethylenimine (PEI) at a 5:1 PEI:DNA ratio in HG-DME medium.

**Plasmids.** The ANT XR1-sv1-HA and ANT XR1-sv2-HA plasmids have been described previously (11). QuickChange site-directed mutagenesis (Stratagene) was used to introduce triple alanine mutations between amino acids 370 and 420 of ANT XR1-sv1 (Table 1 of the Supporting Information). The pEGFP-ANT XR1<sub>360–420</sub> and pEGFP-ANT XR1<sub>360–420</sub>(Y383C) plasmids were made by amplifying amino acids 360–420 from the previously described plasmids, ANT XR1-sv1-HA and

<sup>†</sup>This research was supported by National Institutes of Health Grant RO1 AI067683.

\*To whom correspondence should be addressed: Department of Laboratory Medicine and Pathobiology, Medical Science Building, Rm. 6308, 1 King's College Circle, University of Toronto, Toronto, ON M5S 1A8, Canada. E-mail: jeremy.mogridge@utoronto.ca. Phone: (416) 946-8095. Fax: (416) 978-5959.

<sup>1</sup>Abbreviations: ANT XR, anthrax toxin receptor; PA, protective antigen; sv1, splice variant 1; SDS-PAGE, sodium dodecyl sulfate–polyacrylamide gel electrophoresis.

ANTXR1-sv1-Y383C-HA (11), respectively, using the forward primer 5'-GCGAAGCTTCGGAGGAGAGTGAGGAA-GAAG-3' and the reverse primer 5'-CAAAGAATGCAA-GAGTCAAGATGTAGGCATCC-3'. The PCR products were digested with *Hind*III and *Bam*HI and ligated into pEGFP-C1 (BD Biosciences Clontech).

**Actin Association Assays.** HeLa cells transiently transfected with wild-type ANTXR1 (sv1 and sv2) and ANTXR1 mutants were washed and scraped in PHEM buffer [60 mM PIPES, 25 mM HEPES, 10 mM EGTA, and 2 mM MgCl<sub>2</sub> (pH 6.9)]. Cells were lysed in PHEM buffer with 0.15% Triton X-100 for 12 min at 4 °C. Following lysis, cells were centrifuged at 16000g for 30 min at 4 °C. The soluble fraction was collected, and the pellet (insoluble fraction) was resuspended in equal volumes of PHEM/0.15% Triton X-100 buffer. SDS sample buffer was added to both fractions and the mixture boiled, and equal volumes of each were subjected to SDS-PAGE and Western blotting. Blots were probed with anti-HA antibodies (Santa Cruz, catalog no. E1608) and visualized using a Kodak Image Station 4000MM Pro. The intensities of the bands were quantified, and the ANTXR1 ratio in the pellet to supernatant was determined.

**Fluorescence Microscopy.** HeLa cells were seeded on cover slips and transfected with pEGFP-ANTXR1<sub>360-420</sub>, pEGFP-ANTXR1<sub>360-420</sub>(Y383C), or pEGFP plasmids. Cells were washed twice in phosphate-buffered saline (PBS) and fixed in 4% paraformaldehyde in PBS for 15 min at room temperature. Cells were then washed two more times with PBS, permeabilized with 0.2% Triton X-100 in PBS for 5 min, washed four times with PBS, and blocked in 5% BSA in PBS for 30 min at room temperature. Cells were stained with 5 units/mL Alexa555-Phalloidin (Molecular Probes) in 5% BSA for 1 h in the dark at room temperature. Following staining, cells were washed three times with PBS and mounted on glass slides. To visualize actin and EGFP signals, conventional fluorescence microscopy was performed on Zeiss Axioplan 2 and the images were compiled using AxioVision LE.

**ANTXR1 Peptides and Actin Preparations.** The TAIL<sub>360-420</sub> peptide containing amino acids 360–420 of human ANTXR1-sv1 and an amino-terminal biotin tag was synthesized (AnaSpec Inc.). TAIL<sub>360-420</sub>(Y383A) is identical to TAIL<sub>360-420</sub> except for a tyrosine to alanine substitution corresponding to ANTXR1-sv1 position 383. TAIL<sub>360-420</sub> and TAIL<sub>360-420</sub>(Y383A) were incubated with streptavidin-agarose resin at a concentration of 4 mg of peptide/mL of resin and rotated for 30 min at room temperature in EBC buffer [50 mM Tris (pH 8), 120 mM NaCl, 0.5% (v/v) NP-40, and 50 µg/mL phenylmethanesulfonyl fluoride]. Peptide-bound streptavidin-agarose beads were centrifuged at 1500g for 5 min and resuspended in equal volumes of EBC buffer.

For ANXTR1 peptide experiments and native gel electrophoresis, purified human  $\beta$ -actin (Cytoskeleton Inc., Catalog no. APHL95) was diluted and depolymerized in general actin buffer [0.2 mM CaCl<sub>2</sub> and 5 mM Tris (pH 8), supplemented with 0.2 mM ATP] at a concentration of 0.5 mg/mL for 45 min at room temperature and centrifuged at 16000g for 30 min to remove residual nucleating centers. For electron microscopy experiments, 0.5 mg/mL  $\beta$ -actin in general actin buffer was depolymerized as described above, followed by addition of 10 $\times$  actin polymerization buffer [Cytoskeleton Inc., catalog no. BSA02 (500 mM KCl, 20 mM MgCl<sub>2</sub>, and 10 mM ATP)] diluted to a 1 $\times$  concentration, and incubated for 1 h at room temperature to stimulate filament formation.

**ANTXR1 Peptide Experiments.** HeLa cells were washed three times and scraped in PBS. Cells were lysed in EBC buffer by being rotated for 1 h at 4 °C, and lysates were cleared by centrifugation, followed by determination of protein concentrations by the Bradford assay. Either 50 µL of TAIL<sub>360-420</sub> or TAIL<sub>360-420</sub>(Y383A) peptide-bound streptavidin-agarose beads (50% slurry) was added to 2 mg of cell lysates and rotated for 2 h at 4 °C. After incubation, beads were washed three times in EBC buffer, and proteins were eluted using SDS loading dye. Eluted proteins were subjected to SDS-PAGE and Western blotting. Blots were probed for  $\beta$ -actin (Sigma, catalog no. A5441). To ensure equal levels of each peptide were used, blots were stripped and reprobed with anti-streptavidin HRP-conjugated antibodies (Pierce, catalog no. 21126) to detect the biotin-labeled peptides.

To investigate direct binding between ANTXR1 peptides and  $\beta$ -actin, 50 µL of peptide-bound streptavidin-agarose beads was incubated with 5 µg of monomeric  $\beta$ -actin and rotated for 2 h at 4 °C. Beads were then washed three times with EBC buffer, and proteins were eluted and subjected to SDS-PAGE and Western blotting for  $\beta$ -actin as described above.

**Native Gel Electrophoresis.** Monomeric  $\beta$ -actin (10 µM) was incubated alone or with 2, 10, or 50 µM TAIL<sub>360-420</sub> or TAIL<sub>360-420</sub>(Y383A) for 15 min in a total volume of 12 µL. The mixtures were run on a 4 to 20% polyacrylamide gel (Bio-Rad), and proteins were visualized with SimplyBlue SafeStain (Invitrogen).

**Electron Microscopy.**  $\beta$ -Actin filaments polymerized from 10 µM monomeric actin were incubated with or without 10 µM TAIL<sub>360-420</sub> or TAIL<sub>360-420</sub>(Y383A) in general actin buffer for 30 min at room temperature. After incubation, samples were applied to carbon-coated 0.25% Formvar films (in dichloroethane) and negatively stained with 2% phosphotungstate acid (PTA) in dH<sub>2</sub>O (pH 6.9). Electron micrographs were recorded using a Hitachi H-7000 transmission electron microscope in the Microscopy Imaging Laboratory at the University of Toronto.

## RESULTS

Triple alanine substitutions were introduced into ANTXR1-sv1 within a 50-amino acid cytoplasmic region, which is conserved between ANTXR1-sv1 and ANTXR2, to define the region within the cytoplasmic tail of ANTXR1-sv1 that mediates its interaction with the actin cytoskeleton. HeLa cells were transiently transfected with wild-type and mutant ANXTR1 HA-tagged fusion proteins. The cells were lysed and sedimented such that cytoskeleton-associated receptors were predominantly pelleted and receptors not associated with the cytoskeleton remained in the supernatant. We have used this assay previously to demonstrate that ANTXR1-sv1 associates with the actin cytoskeleton, whereas ANTXR1-sv2 does not (11). ANTXR1-sv1 mutants containing triple alanine substitutions between amino acids 379 and 411 were found predominantly in the supernatant, suggesting that this 33-amino acid region is necessary for the association of ANTXR1-sv1 with the actin cytoskeleton (Figure 1). Substitution of amino acids 373–375 or 376–378 with alanines had a more modest effect; the two mutant receptors were almost equally partitioned between the pellet and supernatant fractions. In contrast, flanking mutations (370–372, 412–414, 415–417, and 418–420) did not alter the sedimentation properties of the receptor.

To determine whether this region of ANTXR1-sv1 was sufficient to interact with the actin cytoskeleton, we transiently expressed in HeLa cells the EGFP fusion proteins EGFP-ANTXR1<sub>360-420</sub>

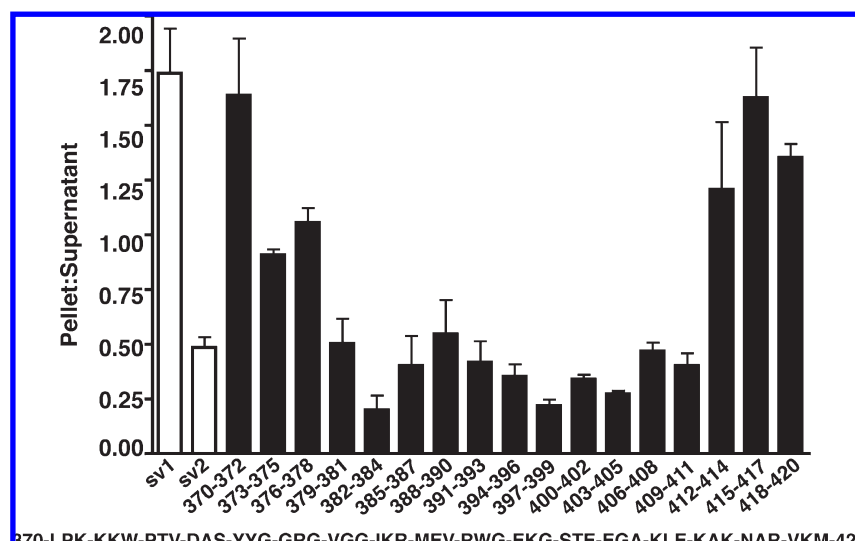


FIGURE 1: Mutations in the cytoplasmic domain of ANT XR1-sv1 impair cytoskeleton association. ANT XR1-sv1-HA and ANT XR1-sv2-HA (white bars) and ANT XR1-sv1-HA triple alanine mutants (black bars) were individually expressed in HeLa cells. The cells were lysed, and the cellular lysates were centrifuged for 30 min. The ratio of the amount of receptor that sedimented to the amount that remained in the supernatant was quantified. The sequence of a segment of the ANT XR1-sv1 cytoplasmic tail is indicated. Error bars indicate the standard error of the mean of three independent experiments.

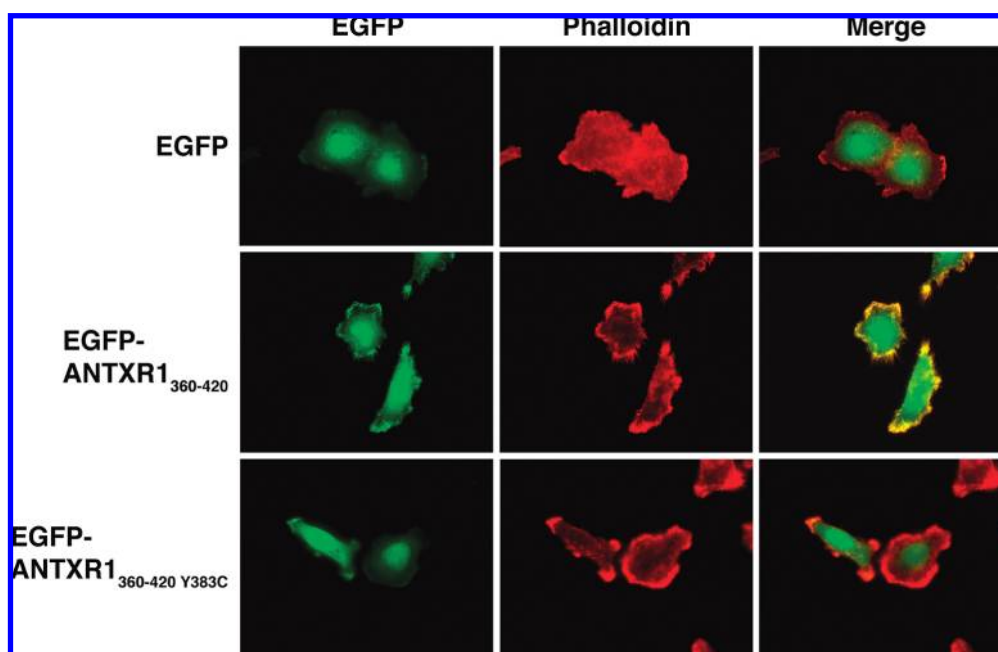


FIGURE 2: ANT XR1<sub>360-420</sub> localizes to actin-rich regions of the cell. HeLa cells were transfected with pEGFP, pEGFP-ANT XR1<sub>360-420</sub>, or pEGFP-ANT XR1<sub>360-420</sub>(Y383C) (left panels, green) and stained with Alexa555-Phalloidin to visualize actin (middle panels, red). Right panels show merged images with colocalization indicated in yellow. Images are representative of ~25 cells from four independent experiments.

and EGFP-ANT XR1<sub>360-420</sub>(Y383C) and stained the cells with Alexa555-Phalloidin to visualize actin. EGFP-ANT XR1<sub>360-420</sub> localized to actin-rich regions of the cell, including protrusions that resembled filopodia (Figure 2). In contrast, EGFP and EGFP-ANT XR1<sub>360-420</sub>(Y383C), which contains a mutation that disrupts the interaction between ANT XR1-sv1 and the cytoskeleton (11), did not localize to the actin-rich periphery of the cell. These results indicate that amino acids 360-420 of ANT XR1-sv1 are sufficient to bind the cytoskeleton.

We next synthesized peptides based on this region, TAIL<sub>360-420</sub>, and TAIL<sub>360-420</sub>(Y383A). A biotin tag was incorporated at the N-terminus of the peptides to facilitate binding to streptavidin-agarose resin. The peptide-bound resin was incubated with HeLa

cell lysates, and the associated proteins were subjected to SDS-PAGE and Western blotting with an anti- $\beta$ -actin antibody. We observed that TAIL<sub>360-420</sub> precipitated  $\beta$ -actin from cellular lysates, whereas TAIL<sub>360-420</sub>(Y383A) did not (Figure 3A).

We next tested whether TAIL<sub>360-420</sub> bound actin directly by incubating the peptide with purified human  $\beta$ -actin. This mixture was centrifuged, and the precipitated proteins were subjected to SDS-PAGE. We observed that TAIL<sub>360-420</sub>, but not TAIL<sub>360-420</sub>(Y383A), bound actin (Figure 3B). To further establish the direct interaction between actin and this cytoplasmic region of ANT XR1, we performed native gel electrophoresis using various concentrations of the ANT XR1 peptides incubated in the presence or absence of purified human  $\beta$ -actin.  $\beta$ -Actin



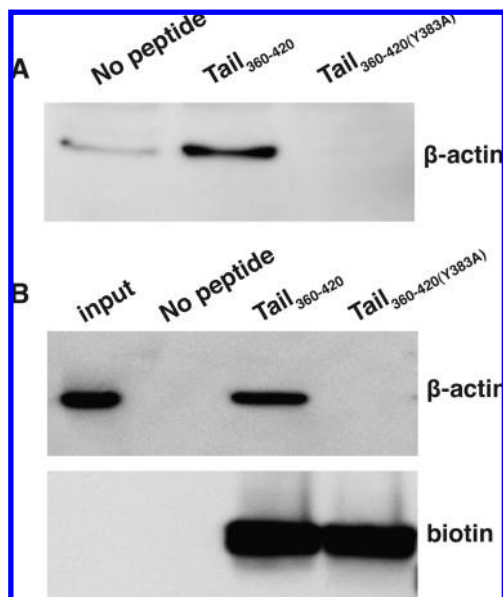


FIGURE 3: Segment of the ANTXR1-sv1 cytoplasmic domain that binds actin. Peptides TAIL<sub>360–420</sub> and TAIL<sub>360–420</sub>(Y383A) were bound to streptavidin beads and incubated with (A) HeLa cell lysates or (B) purified  $\beta$ -actin. The beads were pelleted, and the associated proteins were subjected to SDS–PAGE and transferred to nitrocellulose. Blots were probed for biotin, to detect the peptides, or for  $\beta$ -actin. Blots are representative of three independent experiments.

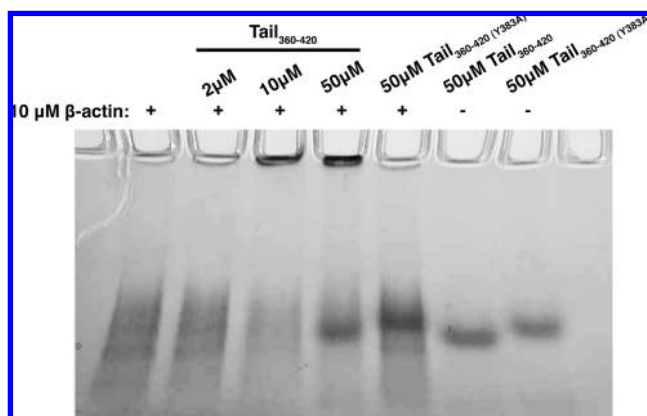


FIGURE 4: Association of  $\beta$ -actin with TAIL<sub>360–420</sub>. Combinations of  $\beta$ -actin, TAIL<sub>360–420</sub>, and TAIL<sub>360–420</sub>(Y383A) were subjected to native gel electrophoresis. Proteins were visualized with SimplyBlue SafeStain. The gel is representative of three independent experiments.

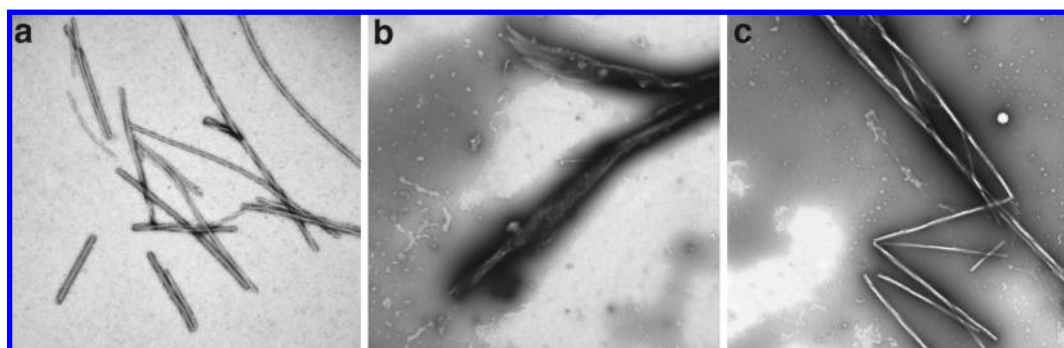


FIGURE 5: TAIL<sub>360–420</sub> bundles actin filaments. Electron micrographs of  $\beta$ -actin filaments incubated alone (a) or with TAIL<sub>360–420</sub> (b) or TAIL<sub>360–420</sub>(Y383A) (c). Images were taken at 20000 $\times$  magnification, and the scale bar represents 500 nm. Micrographs are representative of three independent experiments.

alone was visualized as a smear in the gel, which progressively decreased in intensity when actin was incubated with increasing concentrations of TAIL<sub>360–420</sub> (Figure 4). The decrease in the actin smear was accompanied by the appearance of a band that only just entered the gel, which could represent a large protein complex. In contrast, no detectable change in the mobility of actin was observed when actin was incubated with TAIL<sub>360–420</sub>(Y383A) (Figure 4).

As the native gel electrophoresis data suggested large complexes could be forming between actin and TAIL<sub>360–420</sub>, we were interested in whether this peptide promoted actin filament polymerization. As determined by transmission electron microscopy, incubation of monomeric  $\beta$ -actin with TAIL<sub>360–420</sub> led to the formation of disorganized actin aggregates, which were absent when  $\beta$ -actin was incubated in the presence of TAIL<sub>360–420</sub>(Y383A) (data not shown). This observation suggested that TAIL<sub>360–420</sub> does not stimulate polymerization but might cross-link actin monomers.

To test the cross-linking ability of the peptides, we next incubated  $\beta$ -actin filaments (Figure 5A) with TAIL<sub>360–420</sub> and observed by electron microscopy that the filaments became organized into side-by-side arrays or bundles (Figure 5B); we observed no effect on the arrangement of filaments incubated with TAIL<sub>360–420</sub>(Y383A) (Figure 5C). These data suggest this region of the cytoplasmic tail of ANTXR1 bundles filamentous actin.

## DISCUSSION

Here we provide evidence of a direct interaction between the anthrax toxin receptor ANTXR1-sv1 and the actin cytoskeleton. There have been few reports demonstrating direct interactions between the cytoskeleton and single-transmembrane domain receptors. The epidermal growth factor receptor (EGFR) and the Coxsackie and adenovirus receptor (CAR) are notable exceptions (13, 14). It appears, however, that most membrane proteins that bind the cytoskeleton directly are ion channels. The epithelial cell CIC-2 chloride channel is directly linked to the actin cytoskeleton, and this linkage inhibits channel activity (15). Binding of the epithelial sodium channel, ENaC, to the cytoskeleton activates the channel to allow influx of Na<sup>2+</sup> into the cell; elevated intracellular Na<sup>2+</sup> levels then trigger actin to dissociate from ENaC, thereby downregulating channel activity (16).

Our previous work revealed an inverse correlation between the binding of ANTXR1 to the cytoskeleton and the amount of PA bound to receptors on cells, which suggested that the association of the cytoplasmic tail with the cytoskeleton converts the

extracellular I domain to a closed conformation. This process might occur in a manner similar to how signals from the cytoplasm are transmitted to the I domains of integrins: the cytoplasmic domains of integrin heterodimers are pulled apart to disrupt the interaction between the two transmembrane domains, which serves to transmit the signal across the plasma membrane (17). A difference between the ANTXR1 and integrin activation models appears to be that integrins do not bind the cytoskeleton directly and rely on adaptor proteins to mediate inside-out signaling. Whether it is the binding of the cytoplasmic tail of ANTXR1 to actin filaments or bundles that affects I domain conformation is not clear.

Actin bundling proteins organize actin filaments into ordered arrays that play roles in cell shape, adhesion, and motility (18). For example, fascin organizes actin filaments to form cell-protruding structures called filopodia, and  $\alpha$ -actinin increases the stiffness of stress fibers by bundling filaments (19). ANTXR1 and ANTXR2, being ubiquitous membrane proteins, may have distinct activities compared to previously described bundling proteins.

Proteins that organize actin into bundles can possess two distinct actin binding domains or contain a single actin binding domain and a dimerization domain (18). We performed sedimentation equilibrium ultracentrifugation to determine the molecular weights of TAIL<sub>360–420</sub> and TAIL<sub>360–420</sub>(Y383A) and found that the molecular weight of each peptide was within 1% of their predicted monomeric molecular weights (data not shown). This result suggests that the TAIL<sub>360–420</sub> peptide does not form a dimer, so it may have two distinct actin binding surfaces that facilitate actin cross-linking. It should be noted, however, that monomeric proteins possessing a single actin binding domain could induce bundles by facilitating packing of actin filaments (20). Further work is needed to determine how the ANTXR1-sv1 cytoplasmic tail bundles actin.

## SUPPORTING INFORMATION AVAILABLE

Sequences of the oligonucleotides used for site-directed mutagenesis. This material is available free of charge via the Internet at <http://pubs.acs.org>.

## REFERENCES

- Young, J. A., and Collier, R. J. (2007) Anthrax toxin: Receptor binding, internalization, pore formation, and translocation. *Annu. Rev. Biochem.* 76, 243–265.
- Leppla, S. H. (1982) Anthrax toxin edema factor: A bacterial adenylate cyclase that increases cyclic AMP concentrations of eukaryotic cells. *Proc. Natl. Acad. Sci. U.S.A.* 79, 3162–3166.
- Duesbery, N. S., Webb, C. P., Leppla, S. H., Gordon, V. M., Klimpel, K. R., Copeland, T. D., Ahn, N. G., Oskarsson, M. K., Fukasawa, K., Paull, K. D., and Vande Woude, G. F. (1998) Proteolytic inactivation of MAP-kinase-kinase by anthrax lethal factor. *Science* 280, 734–737.
- Bell, S. E., Mavila, A., Salazar, R., Bayless, K. J., Kanagala, S., Maxwell, S. A., and Davis, G. E. (2001) Differential gene expression during capillary morphogenesis in 3D collagen matrices: Regulated expression of genes involved in basement membrane matrix assembly, cell cycle progression, cellular differentiation and G-protein signaling. *J. Cell Sci.* 114, 2755–2773.
- Hotchkiss, K. A., Basile, C. M., Spring, S. C., Bonuccelli, G., Lisanti, M. P., and Terman, B. I. (2005) TEM8 expression stimulates endothelial cell adhesion and migration by regulating cell-matrix interactions on collagen. *Exp. Cell Res.* 305, 133–144.
- Nanda, A., Carson-Walter, E. B., Seaman, S., Barber, T. D., Stampfl, J., Singh, S., Vogelstein, B., Kinzler, K. W., and St Croix, B. (2004) TEM8 interacts with the cleaved C5 domain of collagen  $\alpha$ 3(VI). *Cancer Res.* 64, 817–820.
- Liu, S., Crown, D., Miller-Randolph, S., Moayeri, M., Wang, H., Hu, H., Morley, T., and Leppla, S. H. (2009) Capillary morphogenesis protein-2 is the major receptor mediating lethality of anthrax toxin in vivo. *Proc. Natl. Acad. Sci. U.S.A.* 106, 12424–12429.
- Cullen, M., Seaman, S., Chaudhary, A., Yang, M. Y., Hilton, M. B., Logsdon, D., Haines, D. C., Tessarollo, L., and St Croix, B. (2009) Host-derived tumor endothelial marker 8 promotes the growth of melanoma. *Cancer Res.* 69, 6021–6026.
- Hanks, S., Adams, S., Douglas, J., Arbour, L., Atherton, D. J., Balci, S., Bode, H., Campbell, M. E., Feingold, M., Keser, G., Kleijer, W., Mancini, G., McGrath, J. A., Muntoni, F., Nanda, A., Teare, M. D., Warman, M., Pope, F. M., Superti-Furga, A., Futreal, P. A., and Rahman, N. (2003) Mutations in the gene encoding capillary morphogenesis protein 2 cause juvenile hyaline fibromatosis and infantile systemic hyalinosis. *Am. J. Hum. Genet.* 73, 791–800.
- Werner, E., Kowalczyk, A. P., and Faundez, V. (2006) Anthrax toxin receptor 1/tumor endothelium marker 8 mediates cell spreading by coupling extracellular ligands to the actin cytoskeleton. *J. Biol. Chem.* 281, 23227–23236.
- Go, M. Y., Chow, E. M., and Mogridge, J. (2009) The cytoplasmic domain of anthrax toxin receptor 1 affects binding of the protective antigen. *Infect. Immun.* 77, 52–59.
- Wegener, K. L., Partridge, A. W., Han, J., Pickford, A. R., Liddington, R. C., Ginsberg, M. H., and Campbell, I. D. (2007) Structural basis of integrin activation by talin. *Cell* 128, 171–182.
- den Hartigh, J. C., van Bergen en Henegouwen, P. M., Verkleij, A. J., and Boonstra, J. (1992) The EGF receptor is an actin-binding protein. *J. Cell Biol.* 119, 349–355.
- Huang, K. C., Yasrael, Z., Guerin, C., Holland, P. C., and Nalbantoglu, J. (2007) Interaction of the Cocksackie and adenovirus receptor (CAR) with the cytoskeleton: Binding to actin. *FEBS Lett.* 581, 2702–2708.
- Ahmed, N., Ramjeesingh, M., Wong, S., Varga, A., Garami, E., and Bear, C. E. (2000) Chloride channel activity of ClC-2 is modified by the actin cytoskeleton. *Biochem. J.* 352 (Part 3), 789–794.
- Mazzochi, C., Benos, D. J., and Smith, P. R. (2006) Interaction of epithelial ion channels with the actin-based cytoskeleton. *Am. J. Physiol.* 291, F1113–F1122.
- Ginsberg, M. H., Partridge, A., and Shattil, S. J. (2005) Integrin regulation. *Curr. Opin. Cell Biol.* 17, 509–516.
- Winder, S. J., and Ayscough, K. R. (2005) Actin-binding proteins. *J. Cell Sci.* 118, 651–654.
- Le Clainche, C., and Carlier, M. F. (2008) Regulation of actin assembly associated with protrusion and adhesion in cell migration. *Physiol. Rev.* 88, 489–513.
- Tang, J. X., Ito, T., Tao, T., Traub, P., and Janmey, P. A. (1997) Opposite effects of electrostatics and steric exclusion on bundle formation by F-actin and other filamentous polyelectrolytes. *Biochemistry* 36, 12600–12607.